Available online at www.sciencedirect.com

ScienceDirect

Procedia Manufacturing 35 (2019) 980–985

Procedia MANUFACTURING

www.elsevier.com/locate/procedia

2nd International Conference on Sustainable Materials Processing and Manufacturing

(SMPM 2019)

Tillage Condition Effects on Soil/Plow-breast Flow Interaction of a Horizontally Reversible Plow

Feng Luo[a,b], Lin Zhu[a,b*], Min Wei[a,b], Jia-Wen Zhang[a,b], De-Quan Zhu[b], Tien-Chien Jen[b,c]

[a]*Lab of Mechanical Structure & Biomechanics, School of Engineering, Anhui Agricultural University, Hefei, 230036, China*
[b]*Mechanical Engineering Department, School of Engineering, Anhui Agricultural University, Hefei, 230036, China*
[c]*Mechanical Engineering Science Department, University of Johannesburg, Johannesburg, 2006, South Africa*

Abstract

The horizontally reversible plow (HRP) is commonly utilized because of higher performances than the regular mold-board plow. Soil/plow surface flow interaction during HRP tillage trends to incur so severe pressure on the plow-breast as to reduce the plow life. This paper numerically characterized the soil/plow-breast flow interaction and subsequently assessed tillage-condition effects on the plow-breast surface. These tillage conditions herein involved tool speed and operation-al depth. The simulations showed that for either tool speed or operational depth the maximum pressure appeared at the plow-shank of the plow-breast and that the soil pressures were increased with them. The computational fluid dynamics (CFD) based predictions qualitatively agreed with the preliminary experimental results at the identified settings with scanning electronic microscopy. Once again, CFD analysis is demonstrated to be feasible and effective enough to provide insight into improve the horizontally reversible plow by predicting real soil behaviors.

Peer-review under responsibility of the organizing committee of SMPM 2019.

Keywords: Flow interaction; Tool speed; operational depth; Computational fluid dynamics (CFD); Plow-breast

1. Introduction

The aim of tillage contributes to appropriate growth conditions for plant by cutting, breaking, inverting and moving soil layers. Tillage is considered to be the most energy–consuming process in the agricultural engineering [1]. The mold-board plow is a common kind of tillage tool and its plowshare and moldboard are the two main soil-engaging components. The severe soil-tool interaction strongly influences the wear on plow-surface, most especially on either

* Corresponding author. Tel.:+86-13696544372, +011 559 4208 Prof Zhu and Prof Jen are co-corresponding authors

E-mail address: zl009@mail.ustc.edu.cn

2351-9789
Peer-review under responsibility of the organizing committee of SMPM 2019.
10.1016/j.promfg.2019.06.045

plowshare or plow-breast, and contributes to the reduced tool service life. The soil pressure patterns and distributions over the plow surface are associated with the appearance of abrasive wear [2]. Determination of the maximum pressure on the plow surface is therefore of importance.

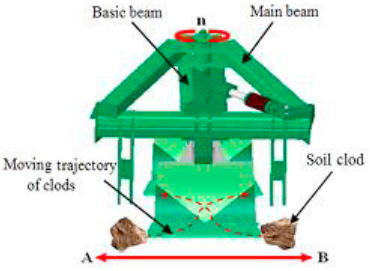

Fig.1.Commuting tillage process of HRP

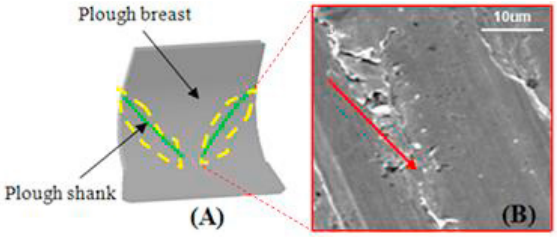

Fig.2. (A) Plow-surface of HRP, (B) SEM micrographs of the worn plow-breast at a tool speed = 1.67 ms^{-1} and an operational depth =0.27m

HRP is a novel moldboard plow designed by the Xin-Jiang Agricultural Mechanization Institute (XJAMI) of China. The unique advantage of HRP is that it can facilitate continuous and alternative commuting tillage. Consequently, it is able to till and cut soil more steadily and orderly than the regular mold-board plow [3].Figure 1 shows the real tillage operation of HRP, where letters A and B both indicate the two different limited tillage locations, the pink dashed curves show the hypothesized flow of soil clods on the plow surface and n is the rotational speed of the basic beam (BB) respect to the main beam (MB) [4].

Actually, severe abrasive wear is always found on the plow surface and most especially on either plowshare or plow-breast after HRP is operated for a certain period. These worn lands can change initial shapes of the plow surface, thereby shortening the tool service life and influencing the plow quality [5]. Figure 2 shows the wear area, measured by a Hisomet II Toolmaker's microscope, at the plow-shank of the plow-breast at a tool speed of 1.67 ms^{-1} and an operational depth =0.27m after 50 ha was plowed. For HRP design optimizing, an underlying mechanism on the soil/ plow-breast interaction is essential to alleviate the worn land that appears on the plow-shank. For this reason, this paper was focused on CFD-based analysis for investigating the soil/plow-breast flow interaction and examining the worn land.

2. Materials and Methods

2.1. Plow-breast geometry

The plow-breast of the HRP, as shown in Fig.2, is a curved surface. For the plow-breast, the overall dimensions related to the soil-tool interaction are 0.567 m in length, 0.008 m in width and a 0.436 m in height (Fig.3) [6]. In the practical tilling operations, the aforementioned geometric parameters of the plow body are actually dependent of the tillage condition and the operating performance. Consequently, they often have influences on the ploughing quality [7]. In this regard, an accurate three-dimensional (3D) plow-breast model is therefore of particular importance to thoroughly assess the soil/plow-breast interaction under real field conditions. In this study, a combination of feature-based approach and scanning technique, previously employed in [8], was applied for the construction of the three-dimensional (3D) plow-breast geometry.

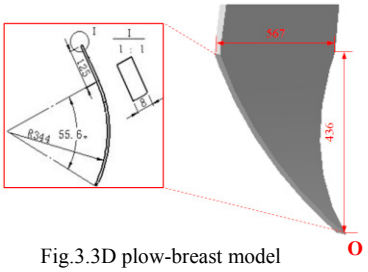

Fig.3.3D plow-breast model

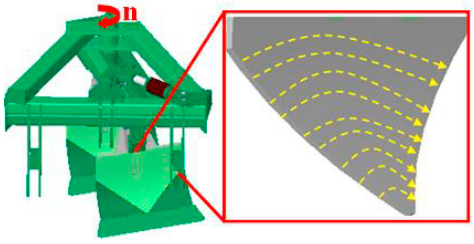

Fig.4 Soil/plow-breast dynamics flow interaction

2.2. Three-dimensional CFD analysis

2.2.1 Dynamics modeling

Figure 4 schematically shows the soil/plow-breast dynamics flow interaction as the HRP implements a tillage action from right to left. Following the real flow configuration, the plow-breast may be acted as a stationary tool located within a visco-plastic flowing domain. This domain represents the soil. Thus, the plow-breast in the free surface domain is comparably a bluff body obstruction. Note that the primary flow domain of the soil on the plow-breast is a surface with an area 0.0924 m^2 (the yellow arrow zone in Fig.4).

2.2.2 Boundary conditions

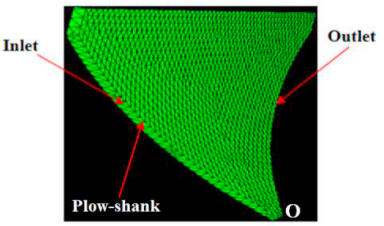

Fig.5.CFD modeling of the plow-breast

In this study, the control volume method was used to predict the pressure distributions and patterns over the plow-breast of HRP in commercial software, i.e., ANSYS Fluent 14.0 (ANSYS FLUENT).Different tool speeds, operational depths and isothermal conditions were all considered for all simulations. Figure 5 illustrates the CFD grid of the tool with 6615 tetrahedral cells in Gambit 2.4(ANSYS FLUENT).

According to the HRP real tillage operation shown in Fig.1, firstly, the soil enters the plow-breast via the left plow-shank with an inlet velocity and subsequently leaves the plow-surface through the right plow-shank (see the yellow arrows in Fig.4). In this regard, we specified the following boundary conditions for CFD simulations: 1) the inlet speed component perpendicular to the plow-shank boundary was 2-8 ms^{-1}, 2) the pressure boundary was applied at the outlet, 3) no slip occurred at the wall boundaries, i.e. at both bottom and side, of the plow-breast, and 4) the free-surface grid movement was only used within the 3D plow-breast surface. Besides, the effects of the different operational depths of HRP, i.e., H = 0.1, 0.2 and 0.3m were also considered according to the relationship between ploughing speed and tillage depth referred by [6]. For all calculations presented here, the solution convergence was judged in accordance with the residuals of the governing equations. That is, all the calculations are stopped and remain stable as the residual of each equation is smaller than 1.0×10^{-5}.

2.2.3 Soil parameters

As depicted above, since real soil contains water and air, multiphase fluid approach is generally used. For simplicity, however, in this work a single-phase laminar flow was applied for the analysis of the soil/ plow-breast flow behaviors. Based on the local soil properties (bulk density—1453 kg/m^{-3}, cone index—398 kPa and moisture content—17%) in Xin-Jiang of China, the soil presented here was modeled as an incompressible, isotropic and homogeneous Bingham material [7]. For CFD modeling purpose, we experimentally determined the dynamic characteristic parameters of the soil with the strain-rate based soil torsional rheometer [6]. The measured values were a yield stress of 15.5kPa and an apparent viscosity of 167 kPa s, respectively. Note that for parameters measuring, two independent variables that strongly influence the yield stress and viscosity, i.e., soil moisture content and core index, were considered, respectively.

3. Results and Discussion

Figure 6 shows the CFD-based predictions under the different operational depths, i.e., 0.1, 0.2, and 0.3m and different tool speeds, i.e., 2, 4, 6, and 8 ms^{-1}. The red, green and blue colors presented here indicate the maximum, median and minimum pressure sections over the plow-breast, respectively. We observed that, for the obtained

pressure distribution and pattern, the tool speed was found in reasonably good qualitative agreement with the operational depth. In other words, the maximum pressures both appeared at the plow-shank of the plow-breast. However, a discrepancy in magnitude was noted for the maximum pressure. The detailed values are listed in Table.1.

Table 1. Highest pressures (Pmax) on the plow-breast for different operational depths (H) and different tool speeds (V)

Pmax	H= 0.1 m	H= 0.2 m	H = 0.3 m
V=2 ms^{-1}	8.38 MPa	10.3 MPa	14.5 MPa
V=4 ms^{-1}	16.8 MPa	20.5 MPa	29.0 MPa
V=6 ms^{-1}	25.2 MPa	30.8 MPa	43.6 MPa
V=8 ms^{-1}	33.6 MPa	41.2 MPa	58.2 MPa

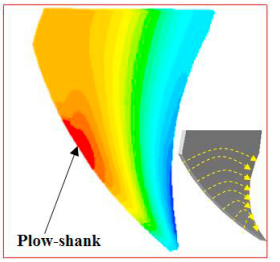

Fig.6 Pressure distribution on the plow-breast for the different operational depths and tool speeds

Figure 7 shows the pressure distributions on the plow-shank with changes in distance at the different operational depths (H), i.e., 0.1, 0.2 and 0.3m. This distance (D) is the vertical distance from any point, e.g., point A of the plow-shank to point O of the plow-breast, as shown in Fig.3.

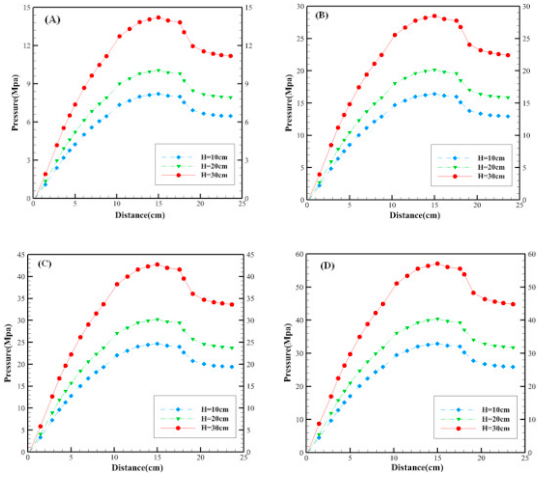

Fig.7 Pressure variation on the plow-shank with change in distance at the different operational depths (H) and a constant tillage speed of (A) 2.0, (B) 4.0, (C) 6.0 and (D) 8.0(ms^{-1})

For the tool speeds of 2 to 8 ms^{-1}, as shown in Fig.7, an increase in the operational depth leads to an increase in the pressure on the plow-shank, and the highest pressures all occur at the intermediary area of the plow-shank. This region is located at the one, approximately ranging from 0.12m to 0.17m, far from point O of the plow-breast (Fig.7). At the operational depths ranging between 0.1 and 0.3m, the maximum pressure approximately increased from 7.8, 16, 24, and 32MPa to 14.4, 29, 43, and 58MPa, respectively, corresponding to the tool speeds of 2, 4, 6 and 8 ms^{-1}. Moreover, for any tillage condition, i.e. operational speed and depth, the pressure on the plow-shank trended to increase to the maximum and then gradually decrease.

Figure 8 plots the pressure variations on the plow-shank with distance at the different tillage speeds, i.e., 2, 4, 6 and 8 ms^{-1}. Note that this distance has the same meaning as in Fig. 7. At three different operational depths of 0.1, 0.2, and 0.3 m, a greater tool speed also contributed to a higher pressure on the plow-shank. Similar to Fig.7, the maximum pressures on the plow-shank also occurred at the center of the plow-shank, about at the zone ranging between 0.12 and 0.17 m. For varying tool speeds of 2 to 8 ms^{-1}, the highest pressures approximately increased from 7, 9, and 14 MPa to 34, 41, and 58 MPa, respectively, corresponding to the operational depths of 0.1, 0.2, and 0.3m. Similar to Fig.7, no matter what either the tool speed or tillage depth is, the pressure variation at the plow-shank was to increase to the maximum first and subsequently gradually decrease.

It can be concluded from Figs. 6~8 that for the different tillage speeds and operational depths, the highest pressures on the plow-breast are all located at the plow-shank zone, more specially at the intermediary area of the plow-shank, where the pressure value is increased as either tillage speed or operational depth is increased. The dominant reason for this trend is that the plow-shank zone is the primary soil engagement zone on the plow-breast. In HRP high-speed tillage processes, a majority of the soil enters the plow-surface by way of the intermittent section of the plow-shank, where a large amount of energy is required cutting, breaking down, inverting the soil layers, and rearranging aggregates. This soil/plow-surface interaction eventually leads to the most severe soil stress gradient at the plow-shank section.

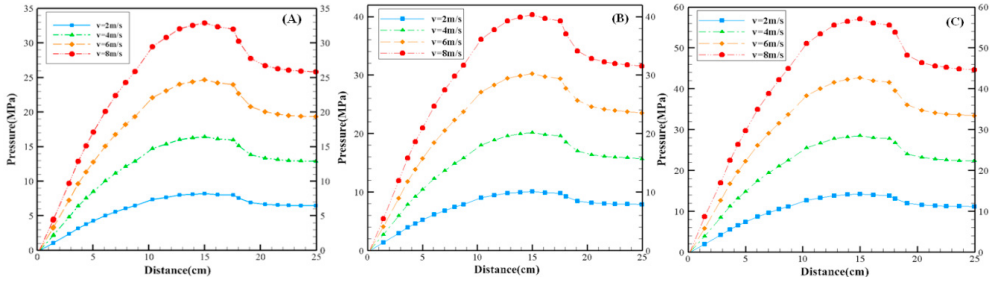

Fig.8. Pressure variation on the plow-breast with change in distance at the different tillage speed (V) and a constant operational depth of (A) 0.1m, (B) 0.2 m and (C) 0.3m.

In the soil-tillage operations, the pressure distribution on the tool surface is directly dependent on the soil front propagation. For the dynamics soil-implement interaction, the foregoing soil flow section is actually a dynamics section exerted by soil stresses [9~11]. For this reason, we inferred that on the plow surface the greatest soil stress indicates the highest pressure. According to [12], a succession of the shear planes tend to cause block separation of the soil mass, which then promotes shear failure to initiate from the primary soil engagement zone of the plow. Hence, we concluded that the greatest load due to the soil-tool interaction lies at the plough-shank zone, numerically demonstrated by CFD modeling in Figs.6~8, and thus supports the assumptions of Coulomb's passive earth pressure theory.

4. Comparison of numerical and preliminary measurements

The CFD-based predictions revealed that the greatest pressures all appeared on the plow-shank section, more especially close to the intermediary area of the shank. Our preliminarily measurements from SEM showed that at a tool speed of 1.67 ms^{-1} and operational depth of 0.27 m, the most severe wear area on the plow-breast occurred on the plow-shank section, too (Fig.2). The area is where the highest pressure at the plow-breast lies (see Figs. 6~8). At the same time, the CFD-based predictions in this study further showed that the highest pressure on the shank zone increased with either tool speed or operational depth. Under similar tillage conditions, for example, when the operational depth was increased from 0.2 m to 0.3 m at a constant tool speed of 2 ms^{-1}, the maximum pressure at the plow-shank was increased from 10.3 MPa to 14.5 MPa (Table.1, Figs. 9(A)~(B)).The recent experimental measurements also demonstrated that at a tool speed of 1.67ms^{-1},a more severely worn area, compared to Fig.2, appeared at the plow-shank when the operational depth was increased from 0.27 m to 0.36 m (see the red arrows in Figs.2 and 9 (C)). Note that this wear area was obtained by using the Hisomet II Toolmaker's microscope too. The highest pressure incurs the most severe wear on the tool surface in the soil cutting operations [13]. Based on the qualitative comparisons among Figs.2, 6 and 9, we conclude that the most severe wear on the tool surface at other operational speeds and depths may also be located at the shank area of the plow-breast, and might be much more severe than the scenario shown in Fig.2.

In conclusion, the CFD-based numerical predictions in the current work show good qualitative agreement with the measurements. These outcomes once again demonstrate that CFD modeling can be feasibly and effectively used to explore the dynamic tillage operations and as a result implement the tool design improvement. However, the obtained results in this study show the forthcoming explorations: 1) the adequate values in the most severe wear area at the shank section, for the different operational speeds and depths, should be calculated in accordance with our acquired greatest pressure profiles, and 2) additional experimental work is required to investigate the worn land on the shank, which includes pressure profile measurements and SEM-based analyses for the same operational parameters. Higher pressure indicates a stronger soil-tool interaction, which in turn leads to more severe wear and

subsequently shortens tool service life.

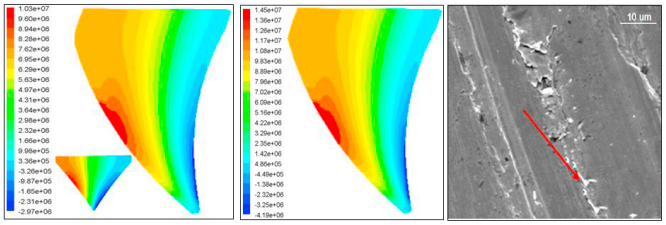

(a) H=0.2 m (b) H=0.3 m (c) H=0.36 m

Fig.9 Comparison between the CFD predictions and the measurements at the similar tillage conditions

5. Conclusions

We proposed here the three-dimensional computational fluid dynamics approach to assess the effects of two important tillage conditions on the soil/plow-breast flow behaviors during the high-speed tillage of the horizontally reversible plow. We demonstrated that the maximum pressures all appeared on the plow-shank section of the plow-surface and that the pressures there were increased with the operational speed and depth. Our preliminary and further measurements also showed that the most severe wear areas appeared at the plow-shank section and the wear areas became more severe with increasing operational depth. It is known that the highest pressure is strongly associated with the most severe wear phenomenon for agricultural tillage tools. Consequently, the CFD-based predictions in this study show good qualitative agreement with the preliminarily measured evidence from SEM. Hence, we once again demonstrate that CFD-based modeling can be feasibly and effectively used for the thorough investigation of soil/plow flow dynamics interactions by predicting real soil behaviors. This method offers a new dimension for HRP design, and any other agricultural tool design.

Acknowledgments

We are grateful to the reviewers for their valuable input. This study was funded by the National NSFC [51575003], the Anhui NSF [1508085ME71] and the graduate student innovation fund of AHAU [2018yjs-58].

References

[1] Ibrahmi, Ayadi, et al. "3D finite element simulation of the effect of mouldboard plough's design on both the energy consumption and the tillage quality." International Journal of Advanced Manufacturing Technology 90.1-4(2017):473-487.

[2] Eltom, A. E. Farid, et al. "Effect of trash board on moldboard plough performance at low speed and under two straw conditions." Journal of Terramechanics 59(2015):27-34.

[3] Lin, Zhu, et al. "Application of Virtual Prototype Technology to Analyzing the Kinetic and Dynamic Characteristics of the Base of the Remote Cylinder." Jsme International Journal 49.1(2006):247-252.

[4] Karmakar, Subrata, and R. L. Kushwaha. "Dynamic modeling of soil–tool interaction: An overview from a fluid flow perspective." Journal of Terramechanics 43.4(2006):411-425.

[5] Shmulevich, I. "State of the art modeling of soil–tillage interaction using discrete element method." Soil & Tillage Research 111.1(2010):41-53.

[6] Lin, Zhu, et al. " Design of plow-breast of Horizontal Reversible Plow with computer simulation technique." Journal of system simulation 20(2008): 3455-3458.

[7] Gill, William R, and G. E. Vanden Berg. "Soil Dynamics in Tillage and Traction. In: Agriculture Handbook No. 316. Agricultural Research Service, U.S. Department of Agriculture, 511." (1967).

[8] Zhu, Lin, et al. "An improved horizontally reversible plow design based on virtual assembly semantics and constraint." Journal of Mechanical Science & Technology 30.1(2016):257-266.

[9] Terzaghi, Karl. "Theoretical Soil Mechanics." Chapman and Hall, London. (1943).

[10] Adachi, K., and N. Yoshioka. "On creeping flow of a visco-plastic fluid past a circular cylinder." Chemical Engineering Science 28.1(1973):215-226.

[11] Lin, Zhu, et al. " Combined finite element and multi-body dynamics analysis of effects of hydraulic cylinder movement on ploughshare of horizontally reversible plough." Soil & Tillage Research 163(2016):168-175.

[12] Anonymous. Earth pressure theory and applications. In: Trenching and Shoring Manual. California Department of Transportation. (2001).Sacramento, USA.

[13] Koolen, Ir. Adrianus Jozef, and I. H. Kuipers. "Agricultural Soil Mechanics." 13(1983).